

New evidences for the fluctuation characteristic of intradecadal periodic signals in length-of-day variation

Hao Ding^{*}, Yachong An, Wenbin Shen

Department of Geophysics, School of Geodesy and Geomatics, Wuhan University, 430079, Wuhan, China

Corresponding address: dhaosgg@sgg.whu.edu.cn

Keypoints

1. A ~ 7.6 yr signal was found in the ΔLOD for the first time.
2. Robust evidences prove that the ~ 5.9 year and ~ 8.5 year in the ΔLOD have no stable damping trends but time-varying amplitudes.
3. Both of the ~ 5.9 year and ~ 8.5 year signals may relative to the jerks, but no evidence can prove that jerks are exactions of them.

Abstract

The intradecadal fluctuations in length-of-day variations (ΔLOD) are considered likely to play an important role in explaining core motions. There are two intradecadal oscillations with ~ 5.9 -year and ~ 8.5 -year periods (referred to as SYO and EYO, respectively) which have been detected in previous studies. But whether the SYO and the EYO have stable damped trends in the 1962 to now time-span and whether the geomagnetic jerks are possible excitation sources for the SYO and the EYO are still debate questions. In this study, based on the same simulation test, the same ΔLOD record and the same method as previous studies, and combined with classic filter method and much longer ΔLOD record, we show robust evidences to prove that the SYO and the EYO have no stable damping trends in the 1962-now time-span, and we confirm that there has an ~ 7.6 yr signal for the first time. After showing that the SYO also has a similar relationship with jerks as pervious study suggested for the EYO, we tend to believe that the SYO and EYO may relative to the geomagnetic jerks. But there is

no robust evidence to show that jerks are possible excitation sources of the SYO or EYO, and none of the SYO and EYO can offer special help in predicting geomagnetic jerks.

Keywords

Intradecadal fluctuations; Length-of-day variations; Damping trends; Geomagnetic jerks

1. Introduction

The fluctuations characteristics and excitations of the intradecadal changes in the ΔLOD were thought to be related with the short-period secular variations in the core geomagnetic field, and hence will help to constrain the strength of the magnetic field in the core and to understand the mechanism of the Earth's core-mantle interacts (e.g., Mound & Buffett, 2006; Gillet et al., 2010; Holme & de Viron, 2012; Gross, 2015). There are two periodic signals have been detected from the ΔLOD in the intradecadal period band (here we mean the 5-10 year period band), an approximately six year oscillation (SYO) (e.g., Liao & Greiner-Mai, 1999; Abarca del Rio et al., 2000; Mound & Buffett, 2006; Holme & de Viron, 2013; Chao et al., 2014; Duan et al., 2015, 2017, 2018; Ding & Chao 2018a,b; Ding 2019; Duan & Huang, 2020a) and an approximately 8.5 year oscillation (EYO) (Ding 2019; Duan & Huang, 2020a). The fluctuation characteristics of those intradecadal changes are thought that can help to determine their possible mechanism (see as Gillet et al., 2010, 2015, 2019). However, the fluctuation characteristics of those two signals are still controversial.

Liao & Greiner-Mai (1999) first found a nearly stable ~ 5.8 year oscillation in ΔLOD in the 1970-1990 (see their Fig. 5a) and found that the Southern Oscillation Index may has some correlation with it. Abarca del Rio et al. (2000) also shown that a 6-7 year oscillation has no stable decreasing trend in the 1900-2000 time-span (see their Figs. 3 and 4), the fluctuation characteristic of it is similar as a modulation suggested by Ding (2019; referred to as D19). Holme & de Viron (2013) shown that the SYO is a stable fluctuation in the 1962-2012 time-span after using an iteratively fitting and removing process. Chao et al. (2014) showed the Morlet Wavelet spectrum of the ΔLOD in the 1962-2012 time-span, their results roughly indicated that the SYO has a decreasing trend from

1965-1997, but change to an increasing trend after 1997 (See their Fig. 1c). After using an Daubechies wavelet low-pass filter and combining with a symmetric extension, Duan et al. (2015) used the normal Morlet wavelet (NMWT) method for the extended ΔLOD time series, and found that the SYO has a nearly stable decreasing trend in the 1962-2012 time-span (see their Fig. 9). Based on the same method and same record (1962-2012), Duan et al (2017) further estimated the quality factor Q of the SYO is 51.6 ± 0.4 based on fitting the envelop curve of the SYO in the time domain. Based on this Q value and a free decay trend for the SYO, Duan et al. (2018) and Duan & Huang (2020b) further considered electromagnetic (EM) coupling at the core-mantle boundary (CMB) under the MICG mechanism. Based on the optimal sequence estimation method (Ding & Shen, 2013; Ding & Chao, 2015a), Ding & Chao (2018a) first found the SYO in global GPS and geomagnetic records and their results shown that the SYO in the ΔLOD , GPS and geomagnetic data have a high degree of consistent synchronicity, and none of them has stable decreasing trend. Based on the AR-z spectrum method (Ding & Chao, 2015b, 2018b), and upon using a much longer ΔLOD time series (1760-2018), Ding (2019) (D19) identified 9 periodic signals, i.e., the ~ 149 year, ~ 68 year, ~ 33 year, ~ 22.3 year, ~ 18.6 year, ~ 13.5 year, ~ 11 year, ~ 8.5 year and ~ 5.85 year periodic signals, in the intradecadal and decadal ranges. They first found that the $\sim 8.5\text{yr}$ periodic oscillation (EYO) and suggested that it can be represented by a stable *cosine* signal. In D19, a clean time series for the SYO was obtained (after fitting and removing the other 8 periodic signals; a similar process as that in Holme & de Viron (2013)), their results showed that the SYO has no stable decay trend in the 1962-2018 time-span, the SYO has a slight decreasing trend in the 1975-1995 time-span, but change to a increasing trend after 1995; this finding is consistent with the result shown in Chao et al. (2014), and D19 explained this by a modulation. Based on Daubechies wavelet fitting, NMWT, and a BEPME (boundary extreme point mirror-image-symmetric extension) method (which was claimed that can avoid the edge effects in the NMWT), Duan & Huang (2020b) (referred as to DH20) analyzed the LOD in the 1962-2019 time-span, their results confirmed that the SYO has a stable decreasing trend and the EYO has a stable increasing trend, and they also confirmed that the SYO has a $Q \sim 51$.

As for the possible relationship between the SYO/EYO and the geomagnetic jerks, Holme & de Viron (2005) first found that the 1969, 1972, 1978, 1982, 1992 and 1999 jerks are well consistent

with the sudden changes in the ΔLOD in the 1962-2005 time-span. Holme & de Viron (2013) further confirmed found that the sudden changes (jumps) in their cleaner SYO time series may give rise to the geomagnetic jerks. Silva et al. (2012) also suggested that the SYO seems to be closely related to some geomagnetic jerks. Chulliat et al. (2015) suggested that the SYO may relative to the 2006, 2009 and 2012 jerks. Soloviev et al. (2017) also suggested that the SYO has some relationship with the 1996, 1999, 2002 and 2014 geomagnetic jerks. D19 first calculated the excitation function time series $\varphi(t)$ for the SYO in ΔLOD based on used a deconvolution process, they found that there is no clear relation between the geomagnetic jerks and $\varphi(t)$, but they concluded that this finding needs to be further confirmed. Duan & Huang (2020b) claimed that they didn't identify any possible excited event for the SYO in 1962-now time-span, and suggested that the SYO is discontinuously excited with a randomly 50-100 year time interval. Upon using 12 selected jerks, DH20 found that the peaks/valleys of the EYO are well consistent with 10 of them, but they suggested that the SYO has no possible relationship with jerks. DH20 further concluded that the EYO can be used to predict jerks.

To date, there two disputes for the SYO and the EYO in the ΔLOD :

- 1) Whether the SYO and the EYO have stable damped trends in the 1962 to now time-span.
- 2) Whether the geomagnetic jerks are possible excitation sources for the SYO and the EYO.

In this study, we try to resolve those two disputes.

2. Whether the SYO and the EYO have stable damped trends

In this section, we will use two ΔLOD time series with different lengths as the datasets, and the ΔLOD time series in Holme & de Viron (2013) and DH20 will be extracted for further using.

2.1 The used datasets

We first extract the residual ΔLOD time series (R_0) and the recovered SYO/EYO (S_1/E_1) from DH20; the SYO time series S_2 from Figure 2 of Holme & de Viron (2013) is also extracted for further comparison.

Furthermore, we choose the 1962-2020 Δ LOD time series from the EOPC04 dataset (Petit & Luzum, 2010), the atmospheric angular momentum (AAM) dataset, the oceanic angular momentum (OAM) dataset and the hydrological angular momentum (HAM) dataset are also chosen for comparing and further using (The AAM/OAM/HAM are the mainly Earth external excitation sources of the Earth's rotation). The 1962-2020 Δ LOD record is firstly decimated (after the low-pass filtering with the 18.263cpy cut-off frequency) from 1 day to 10 days sampling. The AAM record (1948/01-2019/03) (mass terms + motion terms) is also decimated from 6 hours to 10 days sampling. The OAM record (mass terms + motion terms) are combined by two different datasets, ECCO_50yr.oam and ECCO_kf080i.oam; the timespan of the first one is 1949/01/06-2003/01/06 and the sampling is 10 days, the timespan of the second one is 1993/01/02-2019/02/15 and the sampling is daily. We merge them to form a new record with a 1949/01-2019/02 timespan and a 10 days sampling. The HAM record is downloaded from the Special Bureau for Hydrology (based on the Land Surface Discharge Model (LSDM)) (Dill, 2008), the timespan is 1971/01/01-2020/06/04 and the sampling is daily; again, it is decimated from daily to 10 days sampling. The Δ LOD and the AAM/OAM/HAM excited LOD time series are shown in Figure 1a (here we note that the units in the figures of D19 were misspelled to *mas*), their corresponding Fourier amplitude spectra are shown in Figure 1b. We can see that the Δ LOD shorter than 5yr are mainly caused by the AAM effects. All the AAM, HAM and OAM effects have very few contributions to the intradecadal period band (5-10 year), except that the ~5 year signal in the Δ LOD is caused by the AAM (see Figure 1b). Hence, here we only remove the AAM effect from the original Δ LOD time series. The residual Δ LOD time series after removing the AAM effect is referred as G_1 .

As the EOPC04 Δ LOD time series only has a ~58yr length, which may too short to isolate two close signals by using a filter, we further choose a yearly long-term Δ LOD time series (1730-2020) (from: www.iers.org/IERS/EN/Science/EarthRotation/LODsince1623.html?nn=12932).

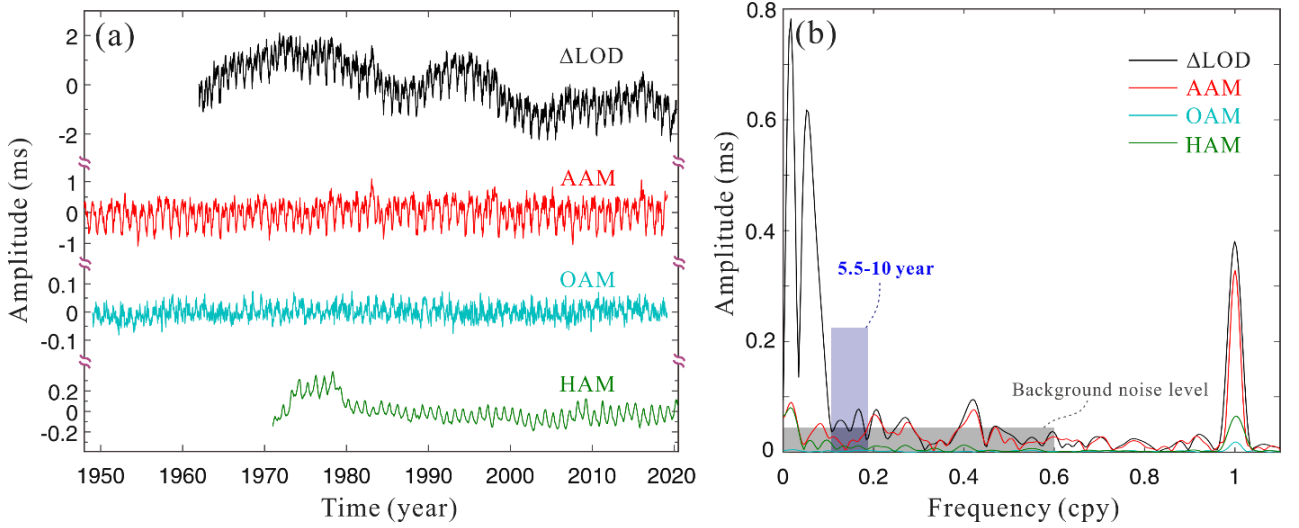


Figure 1. (a) The Δ LOD and the AAM/OAM/HAM excited LOD time series. (b) The corresponding Fourier spectra of the time series in (a); the gray area denotes the background noise level in the 0-0.6cpy, and the blue area denotes the 5.5-10 year period band.

2.2 Reanalysis of the results in previous studies

The extracted R_0 , S_1 and E_1 and their corresponding Fourier spectra are shown in Figs. 1a and 1b (also see Supplementary Fig. S1). The spectra of S_1 and E_1 show clear differences from that of R_0 , and the spectrum of the residual $R_0 - (S_1 + E_1)$ clearly shows a residual peak between the two target signals (see Fig. 1b; the corresponding period is ~ 7 yr). The phases also show clear differences in the target frequency bands (Figs. 1c and 1d). These results preliminarily indicate that the recovered SYO/EYO in DH20 cannot completely represent the real signals in Δ LOD.

When using the classical filtering method for isolating two close signals, the data length should preferably be longer than $2/\Delta f$ (where Δf is the frequency interval). As R_0 is ~ 56 years long, one can safely use a classical high-pass filter to isolate the SYO, but it is not possible to completely filter the ~ 10.6 yr signal (Fig. 1c) for the EYO from R_0 . Here, a residual R_1 is obtained after applying a zero-phase high-pass filter (with a 0.14 cpy cut-off frequency) to R_0 (Fig. 1a). The spectral results show that the SYO amplitude in R_0 and R_1 are almost the same (considering the filtered noise effects; Fig. 1b) and that the phase difference between them is approximately zero (Fig. 1e). These findings mean that the applied filter does not change the real SYO in R_0 . Fig. 1a also shows that the SYO (S_0)

obtained from the filtered G_1 (by using a bandpass filter with 0.14cpy and 0.2cpy as the cutoff frequencies), and the S_2 from Holme & de Viron (2013). We can find that S_0 , S_2 and R_1 have good consistency even though different methods were used (Ding, 2019; Holme & de Viron, 2013), and there has no stable decreasing trend for the SYO in 1962-2019 time-span. In fact, S_1 from DH20 show consistency with R_1 and S_0 only in 1970-2000 time-span (simulation tests also prove this; see Supplementary Fig. S2).

For the EYO, a band-pass filter was applied to the 1730-2020 Δ LOD time series. In the 1962-2019 time-span (Fig. 1a), the EYO is almost a stable oscillation, which is consistent with the finding in D19.

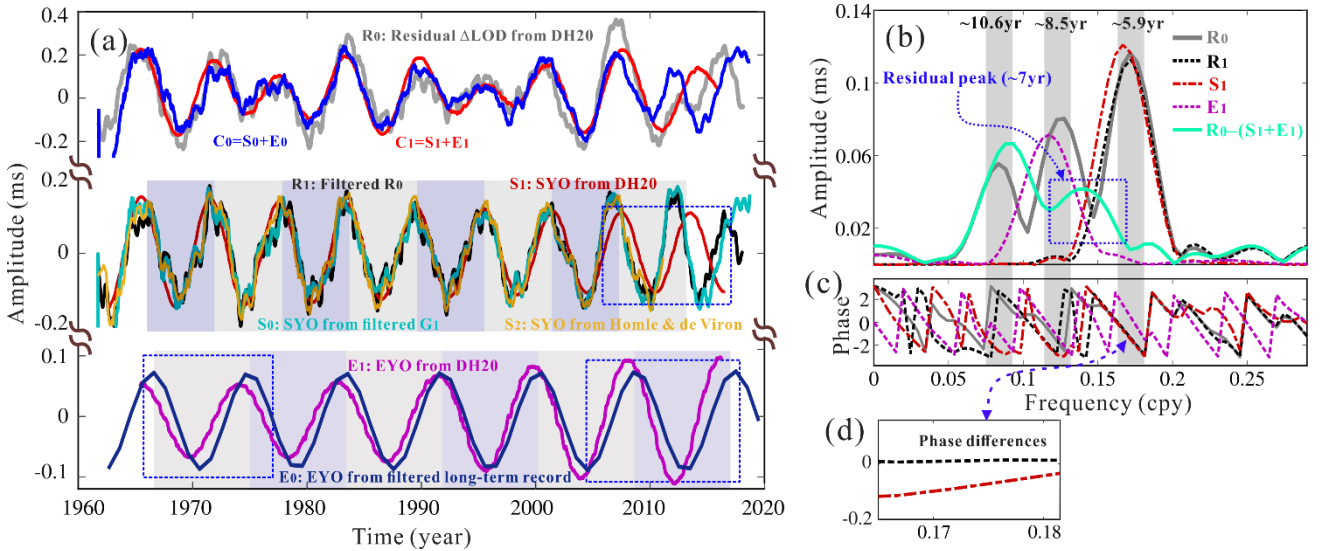


Figure 2. (a) The residual Δ LOD time series (R_0 , gray curve) and the recovered SYO and EYO time series extracted from DH20; R_1 (a filtered version of R_0) and S_0 (SYO from filtered EOPC04 Δ LOD time series) and E_0 (EYO from a long-term Δ LOD record) are also shown. Each of the colored areas in (a) correspond to a fixed 5.9-year (or 8.6-year) period. (b) and (c) The Fourier amplitude and phase spectra of R_0 , R_1 , S_1 , E_1 and $(R_0 - S_1 - E_1)$. (d) The phase differences between R_1/S_1 and R_0 in a narrow frequency band.

The above reanalysis denote that the obtained SYO and EYO by DH20 cannot completely represent the real signals in Δ LOD, and there seems also has a ~ 7.5 yr signal in the 5.5-10yr period band. Besides, both the classic filter result from R_0 and the result from Holme & de Viron (2013)

show that there is no stable decreasing trend for the SYO in 1962-2019 time-span, which is consistent with the finding in D19. The classic filter result for EYO in the 1962-2019 time-span also shows no stable increasing trend.

2.3 New results from classic filter

We first use a high-pass filter to the residual ΔLOD time series G_1 (the cutoff frequency is 0.10cpy), the Fourier spectrum of the filtered G_1 is shown in Fig. 3b (and 3c). Comparing with Fig.2b, we can find that the $\sim 10.6\text{yr}$ signal has been filtered. In the following, we will show that there is actually a $\sim 7.5\text{yr}$ signal in the ΔLOD , not a $\sim 7\text{yr}$ signal. As the length of the filtered G_1 is about 58yr, even there has a $\sim 7.5\text{yr}$ signal, it is still longer enough to filter the SYO from the EYO and the $\sim 7.5\text{yr}$ signal, but it is difficult to isolate the EYO with $\sim 7.5\text{yr}$ signal. Hence, we use a band-pass filter (the cutoff frequencies are 0.148cpy and 0.2cpy) to isolate the SYO from the filtered G_1 (see Fig. 3a), while the EYO is selected from the filtered result that from the 1730-2020 ΔLOD time series (i.e., the time series E_0 in Fig. 2a; also plotted in Fig. 3a). We didn't try to filter the $\sim 7.5\text{yr}$ signal from the 1730-2020 ΔLOD time series, because the amplitude of $\sim 7.5\text{yr}$ seems too small (only $\sim 0.04\text{ms}$) and the data before 1962 are too noise. Instead, we first remove the obtained SYO and EYO from the filtered G_1 , then use an iterative fitting to obtain the $\sim 7.5\text{yr}$ signal. Finally, we find that a 7.6yr periodic signal can well represent this signal (see Fig.3a; green curve).

Fig. 3b shows the Fourier amplitude and phase spectra of the filtered G_1 , SYO+EYO and the residual time series ($G_1 - [\text{SYO} + \text{EYO}]$). The amplitudes and phases around the $\sim 5.9\text{yr}$ show that the obtained SYO can well represent the original spectra, but the results around the $\sim 8.5\text{yr}$ show clear difference between the EYO and the original signal. Similar as Fig. 2b, there is a residual peak around the $\sim 7.5\text{yr}$. Fig. 3c is similar as Fig. 3b, but the fitted 7.6yr signal is input, the results show that the three obtained time series can fully represent the original signals in the 5.5-10yr period band (not only for the amplitude, but also for the phase). Hence, we can conclude that the obtained SYO, EYO and the 7.6yr signal are reasonable. These results also indicate that the SYO and EYO have no stable decay trends.

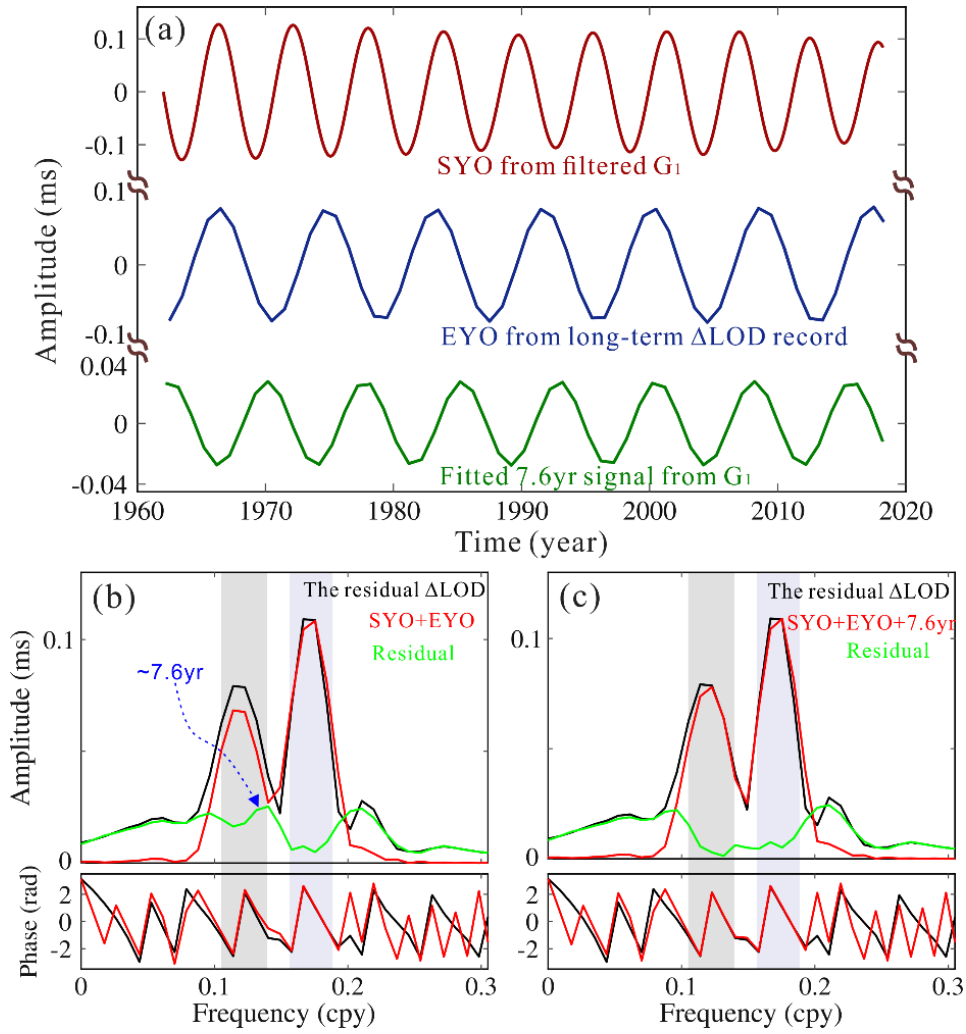


Figure 3. (a) The obtained SYO and EYO from the ΔLOD time series based on the classic filter process; the green curve denotes the fitted 7.6yr signal from the G_1 time series (filtered EOPC04 time series) after removing the SYO and EYO in (a). (b) shows the amplitude and phase spectra for the filtered G_1 and the SYO+EYO (in (a)); the amplitude spectrum for the residual time series (G_1 -SYO-EYO) is also shown in (b). (c) is similar as (b), but further consider the fitted 7.6yr signal.

2.4 Why the decay trends for the SYO and EYO were obtained?

The above sections show that all the results from the classic filter and from Holme & de Viron (2013) have no stable trend for the SYO and EYO, but why do the SYO and EYO recovered in DH20 have stable damping trends? Actually, Supplementary Figs. 3, 9-10, 14 and 15 in DH20 clearly show that the edge effects were still present even when their NMWT+BEPME method was

used. More importantly, their Figs. S14a and S15a show that the recovered signals have clearly increased and slightly decreased amplitudes, respectively, for the simulated stable *sine* signals. In light of this, we may guess that the damping trends for their SYO and EYO results should be affected by their used methods.

We reproduced the same processing strategy explained in DH20 (Daubechies wavelet fitting+NWMT+BEPME) and tested it. Two time series, $S_1(t)$ and $S_2(t)$, were simulated. $S_1(t)$ contains 9 zero-phase and stable *sine* signals (the same as those in DH20, except for the random noise term; see their Supplementary Information); $S_2(t)$ also contains the same 9 periodic signals, but the amplitudes and phases were estimated by fitting the observed ΔLOD (Fig. 4a). The SYO/EYO recovered from $S_1(t)$ (+random noise) are shown in Fig. 4b, and our recovered results are almost the same as those in DH20 (red curve in Fig. 2a) (considering that the random noise cannot be the same). We further used the same process to reanalyze R_0 , and the obtained SYO/EYO almost overlap with the SYO/EYO extracted from DH20 (Fig. 4c; slight differences arise from the errors introduced when extracting data from their figures). Figs. 4b and 4c prove that we have fully reproduced the processing strategy used in DH20.

Given the above, we used the same process to analyze $S_2(t)$. Not surprisingly, we obtained a decreasing SYO and an increasing EYO for the input stable *cosine* signals. As the real observation is more complicated than $S_2(t)$, there is a possibility that even if the SYO/EYO are nearly stable, the NWMT+ BEPME will indicate damping trends for them. Surprisingly, the SYO/EYO recovered from $S_2(t)$ are well consistent with those from the observed ΔLOD (Fig. 4c). Here, we may conclude that the damped nature of the SYO/EYO was only an artifact of the method used in DH20 (more evidence can be obtained from the test codes in the Supplementary Information).

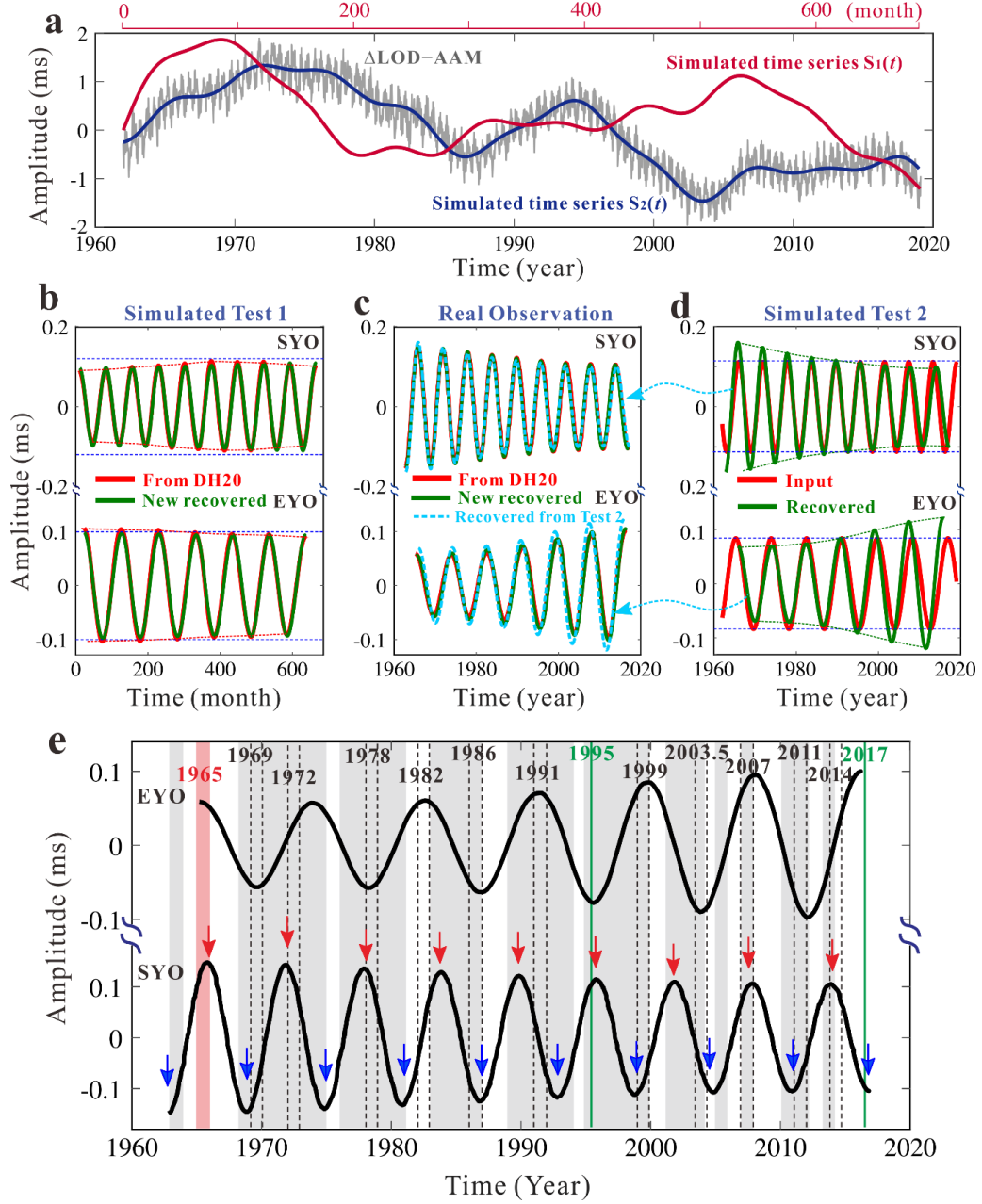


Figure 4. (a) The residual time series G_1 and two simulated records $S_1(t)$ and $S_2(t)$. (b) The SYO and EYO recovered from $S_1(t)$ based on the same processing strategy used in DH20 (Daubechies wavelet fitting+NWMT+BEPME); the SYO and EYO extracted from Figs. S14a/S15b in DH20 are also shown in (b). (c) The SYO and EYO recovered from R_0 based on the same process used in (b). (d) The input SYO/EYO and the recovered SYO/EYO from $S_2(t)$. The SYO/EYO recovered from $S_2(t)$ are potted in (c). (e) The SYO and EYO recovered from DH20 and the jerk events in the past decades. The vertical dashed black lines and the green lines denote the 12 jerks selected in DH20; the grey areas show the jerk bounds from 1957 to 2008, and a new 1965 jerk is added.

3. The relationship between jerks and EYO/SYO

As we have reviewed in section 1, whether the SYO/EYO has some relationships with jerks is a pending problem, although we tend to believe they do have some relationships. In this section, we first follow the thoughts in DH20, i.e., we also compare the damping EYO obtained by DH20 with the jerks, but we will simultaneously compare the damping SYO and we will much more jerks.

In DH20, only 12 jerks were selected, although many jerks have been identified in the past decades. The jerks did not occur at the same time in all regions of the Earth, and they have 1-2 year uncertainty (Brown et al., 2013; Pinheiro et al., 2011; Chulliat & Maus, 2014). Following the inferences of DH20 (although we do not agree), we plotted their recovered SYO/EYO and the 12 selected jerks in Fig. 4e. Among all 12 selected jerks, only the 1972 and 2014 jerks do not correspond to the peaks/valleys of the EYO, but also, only the 1982 and 1991 jerks do not correspond to the peaks/valleys of the SYO. Furthermore, if we refer to the general jerk bounds (Brown et al., 2013) (Fig. 4e), the SYO shows even better consistency with jerks: all of the SYO's valleys are close to the bounds of the jerks. Until now, there is no robust evidence to prove that the EYO must be caused by a torsional oscillation in the fluid outer core, although DH20 have suggested this (as Duan et al. (2018) have suggested for SYO). If the EYO is increased by jerk excitation, as claimed in DH20, why is this not also true for the SYO? Considering that different jerks generally have 1-3 year intervals, the EYO seems to offer no special help in predicting jerks, although we do not rule out the possibility that there will be a jerk in 2020-2021.

In short, if we only simply compare the waveforms of SYO and EYO with jerks in the time domain, Fig. 4e dose show that the SYO/EYO have some relationships with jerks, but more reasonable comparisons should be that comparing the sudden changes in the SYO/EYO time series with jerks or comparing the excitation time series of them with jerks.

4. Discussions and conclusions

The fluctuations characteristics of the SYO and EYO will affect the understanding of their physical mechanisms. In order to confirm them, we reanalyzed the used Δ LOD records in previous studies and further analyzed the EOPC04 Δ LOD time series based on the classic filter process. Our

results shown that the results for SYO from the classic filter process are well consistent with the corresponding results in Holme & de Viron (2013) and Ding (2019) (both of them used a fitting and removing process); meanwhile, the spectra results reveal that the stable damping SYO and EYO given by DH20 are not consistent with their own used Δ LOD record. Besides, we further use the same process (NWMT+BEPME) to further obtain a ~ 7 yr signal from the residual time series ($R_0-S_1-E_1$), a stable increasing time series was obtained (see Supplementary Fig. S3a). This is a strange finding, all the three close signals have stable damped trends. It is difficult to image what physical mechanisms can cause such observations. No matter what, Supplementary Fig. S3b clearly shows that those three time series still cannot represent the amplitude and phase spectra of their used Δ LOD record. Our results from the classic filter process based on the EOPC04 and a much longer Δ LOD time series also show that the SYO and EYO have no stable damping trend. Meanwhile, we confirm that a ~ 7.5 yr signal also present in the Δ LOD time series for the first time (although Hao Ding has fitted and removed ~ 7.7 yr signal in D19 to obtain a much clean SYO time series; this information was not specific explained in D19).

As for the possible relationship between jerks and SYO/EYO, although we don't think that directly comparing the peaks/valleys of the SYO/EYO with jerks is a suitable way, based on this thought, we find that the SYO also has the similar relationship with jerks as DH20 suggested for the EYO. But clearly, there has no evidence to prove that the SYO and EYO were excited by jerks. Further studies are certainly needed. Besides, we add some explanations about the convolution/deconvolution in the SI, which can help other researchers to use the deconvoluted time series of SYO and EYO (i.e., their excitations) to further study on the possible relationship between jerks and SYO/EYO.

Recall the two disputes we summarized in section 1, in this study, we obtain the following conclusions:

- 1) We found a ~ 7.6 yr signal in the EOPC04 Δ LOD time series.
- 2) We confirmed that there are no stable damped trends for the SYO and EYO in the 1962 to now time-span. Instead, both of them have time-varying amplitudes. NWMT+BEPME

methods may cause the strange increasing or decreasing trend for a stable cosine signal when there are many signals contained in the used time series.

- 3) Although the geomagnetic jerks are well consistent with the peaks/valleys of the SYO and EYO, there is no evidence to prove that the jerks are possible excitation sources for the SYO and EYO. Of course, the EYO also cannot be used to predict jerks.

Acknowledgements

We also thank L.T. Liu, X.Q. Su for NMWT algorithm and codes. The used Δ LOD data can be freely downloaded from provided by IERS (<ftp://hpiers.obspm.fr/eop-pc/eop>). This work is supported by NSFC (grant #41974022, 41774024).

References

1. Abarca del Rio, R., Gambis, D. & Salstein, D. A. (2000). Interannual signals in length of day and atmospheric angular momentum. *Annales Geophysicae*, 18(3), 347-364.
2. Brown, W.J., Mound, J.E., & Livermore, P.W. (2013). Jerks abound: an analysis of geo-magnetic observatory data from 1957 to 2008. *Physics of the Earth & Planetary Interiors*, 223, 62-76.
3. Chao, B. F., Chung, W. Y., Shih, Z. R., & Hsieh, Y. K. (2014). Earth's rotation variations: a wavelet analysis. *Terra Nova*, 26(4), 260-264.
4. Chulliat, A., Alken, P., and Maus, S. (2015), Fast equatorial waves propagating at the top of the Earth's core. *Geophys. Res. Lett.*, 42, 3321- 3329. doi: 10.1002/2015GL064067.
5. Chulliat, A., & Maus, S. (2014). Geomagnetic secular acceleration, jerks, and a localized standing wave at the core surface from 2000 to 2010. *Journal of Geophysical Research: Solid Earth*, 119(3), 1531-1543.
6. Dill, R. (2008). Hydrological model LSDM for operational Earth rotation and gravity field variations. *Scientific Technical Report*. 35, STR08/09, GFZ Potsdam, Germany, <https://doi.org/10.2312/GFZ.b103-08095> (2008).
7. Ding, H. (2019). Attenuation and excitation of the ~6 year oscillation in the length-of-day variation. *Earth and Planetary Science Letters*, 507, 131-139.

8. Ding, H., & Chao, B. F. (2018a). A 6-year westward rotary motion in the earth: detection and possible MICG coupling mechanism. *Earth and Planetary Science Letters*, 295, 50-55.
9. Ding, H., & Chao, B. F. (2018b). Application of stabilized AR-z spectrum in harmonic analysis for geophysics. *Journal of Geophysical Research: Solid Earth*, 123, 8249-8259.
10. Ding, H., & Chao, B. F. (2015a). Data stacking methods for isolation of normal-mode singlets of Earth's free oscillation: Extensions, comparisons, and applications. *Journal of Geophysical Research: Solid Earth*, 120(7), 5034-5050.
11. Ding, H., Chao, B. F. (2015b). Detecting harmonic signals in a noisy time-series: the z-domain Autoregressive (AR-z) spectrum, *Geophysical Journal International*, 201(3), 1287-1296.
12. Ding, H., & Shen, W. B. (2013). Search for the Slichter modes based on a new method: optimal sequence estimation. *Journal of Geophysical Research: Solid Earth*, 118(9), 5018-5029.
13. Duan, P. S., & Huang, C. L. (2020a). Intradecadal variations in length of day and their correspondence with geomagnetic jerks. *Nature Communications*, 11(1), 2273.
14. Duan, P. S., & Huang, C. L. (2020b). On the mantle-inner core gravitational oscillation under the action of the electromagnetic coupling effects. *Journal of Geophysical Research: Solid Earth*, 125, e2019JB018863. <https://doi.org/10.1029/2019JB018863>
15. Duan, P. S. Liu, G. Y., Liu, L. T., Hu, X. G., Hao, X. G., Huang, Y., Zhang, Z. M., & Wang, B. B. (2015). Recovery of the 6-year signal in length of day and its long-term decreasing trend. *Earth Planets & Space*, 67(1), 161.
16. Duan, P. S., Liu, G. Y., Hu, X. G., Sun, Y. F., & Li, H. L. (2017). Possible damping model of the 6 year oscillation signal in length of day. *Physics of the Earth & Planetary Interiors*, 265, 35-42.
17. Duan, P. S., Liu, G. Y., Hu, X. G., Zhao, J., & Huang, C. L. (2018). Mechanism of the interannual oscillation in length of day and its constraint on the electromagnetic coupling at the core-mantle boundary. *Earth and Planetary Science Letters*, 482, 245-252.
18. Gillet, N., Jault, D., & Canet, E. (2018). Excitation of travelling torsional normal modes in an earth's core model. *Geophysical Journal International*, 210(3), 1503-1516.

19. Gillet, N., Jault, D., & Finlay, C. C. (2015). Planetary gyre, time-dependent eddies, torsional waves, and equatorial jets at the earth's core surface. *Journal of Geophysical Research Solid Earth*, 120(6), 3991-4013.
20. Gillet, N., Jault, D., Canet, E., & Fournier, A. (2010). Fast torsional waves and strong magnetic field within the earth's core. *Nature*, 465(7294), 74.
21. Gross, R. S. (2015). Earth Rotation Variations - Long Period. *Treatise on Geophysics (Second Edition)*, 3, 215-261.
22. Holme, R., & de Viron, O. (2005). Geomagnetic jerks and a high-resolution length-of-day profile for core studies. *Geophysical Journal International*, 160, 435-439.
23. Holme, R., de Viron, O. (2013). Characterization and implications of intradecadal variations in length of day. *Nature*, 499(7457), 202-4.
24. Liao, D. C., & Greiner-Mai, H. (1999). A new Δlod series in monthly intervals (1892.0 – 1997.0) and its comparison with other geophysical results. *Journal of Geodesy*, 73(9), 466-477.
25. Manda, M., Holme, R., Pais, A., Pinheiro, K., Jackson, A., & Verbanac, G. (2010). Geomagnetic jerks: rapid core field variations and core dynamics. *Space Science Reviews*, 155(1-4), 147-175.
26. Mound, J. E., & Buffett, B. A. (2006). Detection of a gravitational oscillation in length-of-day. *Earth and Planetary Science Letters*, 243(3-4), 383-389.
27. Petit, G. & Luzum, B., 2010. IERS Conventions 2010, IERS Technical Note; 36, Frankfurt am Main: Verlag des Bundesamts für Kartographie und Geodäsie, ISBN 3-89888-989-6.
28. Pinheiro, K. J., Jackson, A., & Finlay, C. C. (2013). Measurements and uncertainties of the occurrence time of the 1969, 1978, 1991, and 1999 geomagnetic jerks. *Geochemistry Geophysics Geosystems*, 12(10). Doi: 10.1029/2011GC003706
29. Silva, L., Jackson, L., Mound, J., 2012. Assessing the importance and expression of the 6 year geomagnetic oscillation. *Journal of Geophysical Research: Solid Earth*, 117, B10101. <https://doi.org/10.1029/2012JB009405>.
30. Soloviev, A., Chulliat, A., Bogoutdinov, S., 2017. Detection of secular acceleration pulses from magnetic observatory data. *Physics of the Earth & Planetary Interiors*, 270, 128–142.

Supplementary Information for
New evidences for the fluctuation characteristic of intradecadal periodic signals in
length-of-day variation

Hao Ding*, Yachong An, Wenbin Shen

*Department of Geophysics, School of Geodesy and Geomatics, Wuhan University, 430079, Wuhan,
China*

Corresponding address: dhaosgg@sgg.whu.edu.cn

Contents of this file

Methods, tests and discussions: The used filter, the parameters for the tests, the example test codes; and discussions about deconvolution.

Figure S1. The original time series in Figs. 1a and 1b of DH20, and our extracted results from them.

Figure S2. Four new simulate tests for validating NWMT+BEPME

Figure S3. The recovered 7yr signal from $R_0 - (S_1 + E_1)$ based on the same process in DH20.

Figure S4. Schematic diagrams for convolution and deconvolution

Methods, tests and discussions

The residual ΔLOD time series R_0 and the recovered SYO and EYO from R_0 for DH20¹ are extracted from their Figs. 1 and 2. We use their original figure as references to show that our extracted time series are almost same as their results. The comparisons between them are shown in Fig. S1.

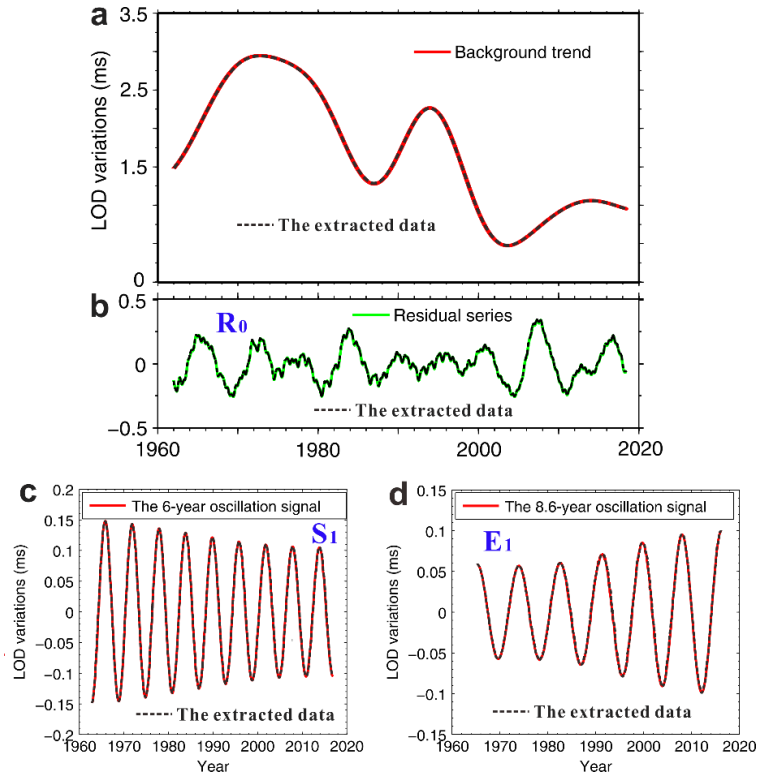


Figure S1. The original time series in Figs. 1a and 1b of DH20, and our extracted results from them (dashed black curves).

In this study, we use a zero-phase digital filter to further filter the R_0 (from DH20 (Duan and Huang, 2020)), the residual ΔLOD time series, and the longer time series. A Matlab code (**DH_filt.m**) for this filter is given (please see the code parts), and the ‘**test_DH_filt_for_SYO_EYO.m**’ can reproduce our results. It is written by Hao Ding, so the readers can freely use it.

As for the process strategy (Daubechies wavelet fitting+NWMT+BEPME) used in DH20, given that we have reproduce the almost same results as theirs from the same simulated test and the same R_0 time series, their process have been reproduced. Actually, both of DH20’s and our core code (NWMT) are based on L.T. Liu’s code, and the BEPME is quite easy to be re-produced. The main difference is that which order of the Daubechies wavelet is used. There are 45 different choices for it in Matlab software, and one can test it in the given test code. We upload three Matlab codes for the simulated tests 1 and 2, *run_simulated_test1.m*, *run_simulated_test2.m* and *nwmt_bepme.p*. The parameters for the two simulated tests in the main test are given in those codes. The readers can use them to reproduce our results and to test other possible cases.

To further show the results from the DH20's process, we do another four simulated tests. Also 9 periodic signals as those in the main test are used, and the amplitudes of them are same as those in the simulated test 2 in the main text, but we randomly choose the phases for them. In Fig. S2, the first two tests consider the stable cosine SYO and EYO, while a decreasing SYO and increasing EYO are inputted in the two last tests. The results from the first two tests are similar as the test 2 in the main test, i.e., a decreasing SYO and increasing EYO are obtained even the inputted signals have stable amplitudes. The last two tests also indicate that results from the (Daubechies wavelet fitting+NWMT+BEPME) process does not similar as DH20 claimed, i.e., their process can well restore a damping oscillation (see simulated test 3 for SYO and simulated test 4 for EYO in Fig. S2).

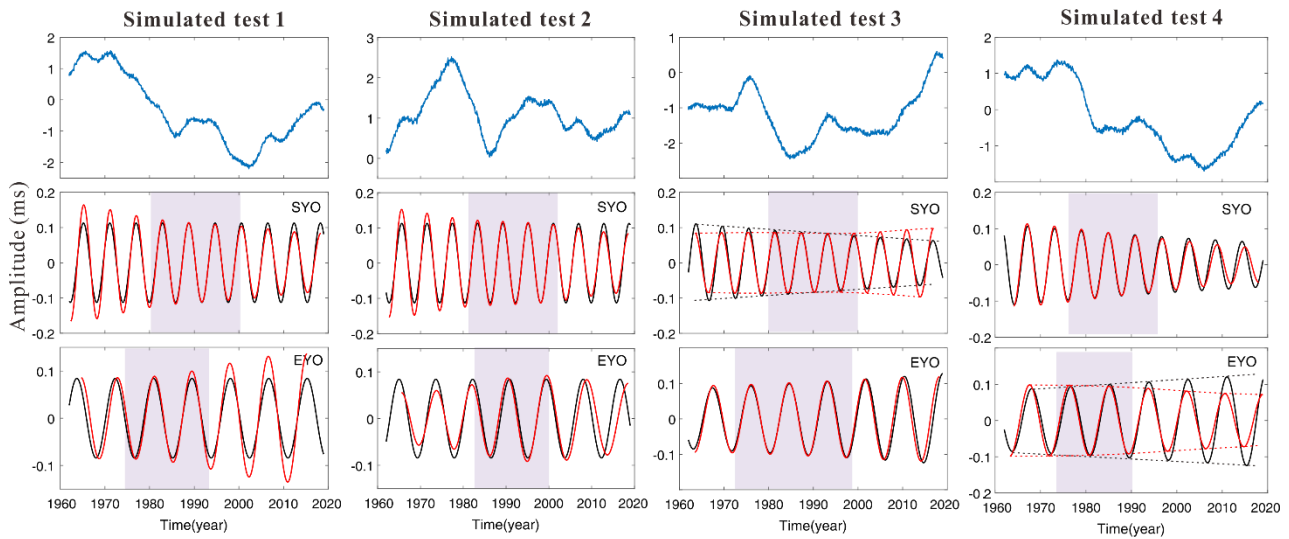


Figure S2. Four new simulate tests for validating NWMT+BEPME. The upper figure in each tests shows the simulated time series, the middle figure and bottom figure for the inputted and recovered SYO and EYO, respectively. The black curves denote the inputted signals and the red curves denote the recovered signals from NWMT+BEPME. The colored areas denote the consistent parts between the inputted and recovered signals.

DH20 (and Duan's other papers) claimed that the BEPME can *avoid* the edge effects in NWMT. But we must say that BEPME seems only can reduce the edge effects of NWMT when the signals contained in the used time series are not too complicate. All the Supplementary Figs. 3, 9, 10, 14 and 15 in DH20 support this (i.e., the edge effects are still presented). From lots of simulated tests, we

find that NWMT+BEPME only has good consistence with the inputted signal between ~1980 to ~2000. If we look at Fig. 1a again in the main text, we will find that the recovered SYO from DH20 also just has good consistence in such time-span with filtered R_0 and S_0 . Fig. S2 also clearly shows that only the 1980-2000 time-span has a slightly decreasing trend, but not for the other time span. Hence, the stable damping SYO and EYO just caused by the BEPME, namely BEPME cannot *avoid* the edge effects of NWMT. We agree with that the NWMT will obtain better results in the middle part of the used record, but obviously disagree with that NWMT+BEPME can obtain the ‘real’ signal in the whole time-span. Even part of the ends were cut in their figures (and our results which similar as them), but their figures still show clearly differences with the inputted ideal signals. Given that their relevant tests use almost same length as the real ΔLOD , recovered results for the two ends will still affected by the edge effects.

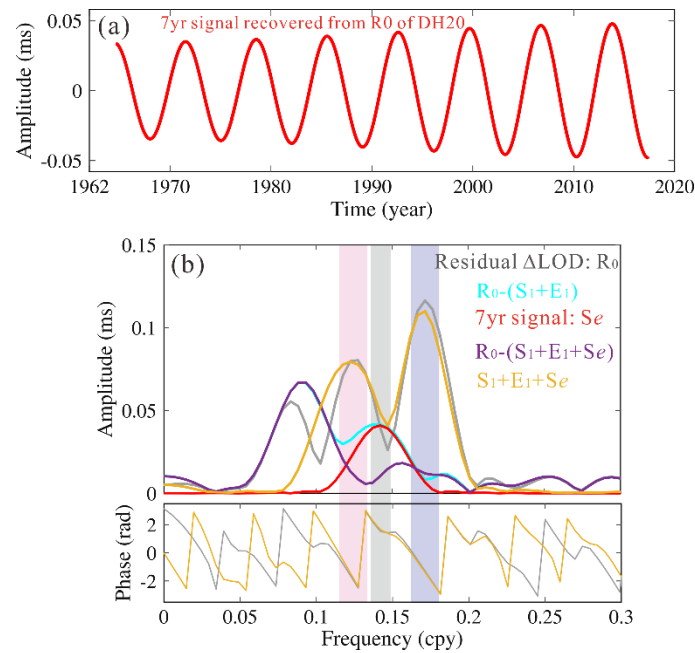


Figure S3. (a) The recovered 7yr signal from the exacted residual time series R_0 after removing the SYO (S_1) and EYO (E_1) based on the same process in DH20. (b) The amplitude and phase spectra of R_0 , the recovered 7yr signal (S_e), $R_0-(S_1+E_1)$, $R_0-(S_1+E_1+S_e)$ and $S_1+E_1+S_e$. (b)The recovered 7yr signal

In order to confirm whether the amplitude and phase deviations between R_0 and S_1+E_1 shown in Fig.2b may be caused by a residual signal, we use the same NWMT+BEPME process to analyze the

residual time series $R_0 - (S_1 + E_1 + Se)$. No surprise, a stable increasing 7yr signal is obtained (see Fig. S3a). Here, we don't judge this result, but suggest the readers to consider the possibility of that three closer signals in the complex Earth system have stable damped trends. Fig. S3b shows that the recovered 7yr signal can represent the spectral amplitude in the residual $R_0 - (S_1 + E_1)$, but the three signals $(S_1 + E_1 + Se)$ clearly cannot well represent the corresponding amplitudes and phases in the residual time series R_0 . This finding means that the amplitude and phase deviations in Fig.2b are not caused by the residual signal. Of course, according the main text, whether the residual peak corresponds to a periodic signal is doubtful, it may be just caused by the un-correct recovered SYO and EYO.

There is another very important thing in the Supplementary of DH20, which will mislead the reader. In their Supplementary 5 and Fig. 18 and 19, DH20 tested the excitations of one/two damping signals by the random noise. In their Supplementary Figs. 18 and 19, two 1000 month long time series convolute with each other, and a 2000 month long (more exactly, 1999 months) 'observed' time series is obtained. Then they claimed that the inputted decreasing signal can be obtained from this 1999 month long time series, but we can find that only last half parts of those 'observed' time series have decreasing trends (see their Supplementary Figs. 18 and 19). Actually, there is a difference between the mathematics and physics, we will explain that only the first 1000 months are the 'real observed' results in physics (Chao, 2017).

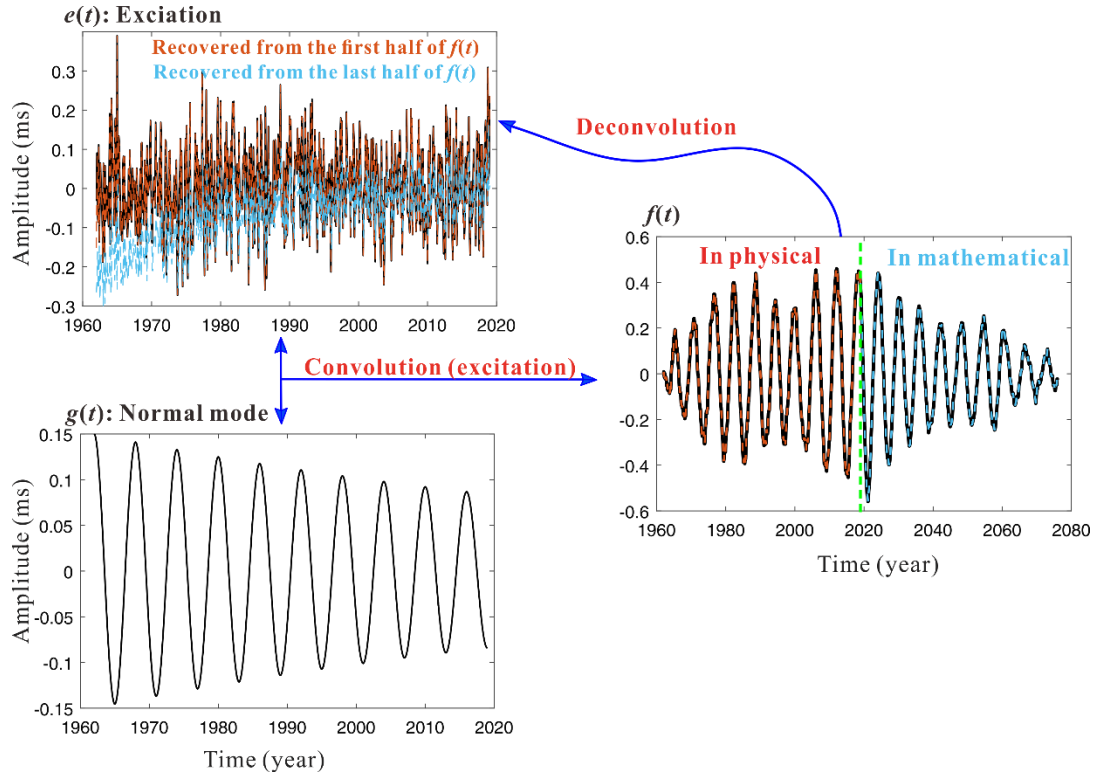


Fig. S4 Schematic diagrams for convolution and deconvolution

Mathematically, if an excitation $e(t)$ convolutes with a normal mode $g(t)$, and they have the same time-span and length N , then a $2N-1$ long time series will be obtained (this is what has shown in DH20). But in the real world, we can only observe the excited changes before now. If one can just use a convolution to obtain the signal after 1000 month later, all phenomena in the world can be easily predicted. However, that's not true. Here we use a simple example to explain this. We simulate an excitation $e(t)$ and a normal mode $g(t)$ in 1962-2019, after convoluting, the 'observed' $f(t)$ can be obtained. For the real world, we only observed the first half of $f(t)$ (the results before the dashed green line in Fig. S4). Suppose we have exactly known the normal mode $g(t)$, then it can be deconvolved from $f(t)$, and we only need the 'real observed' first half part of $f(t)$, the $e(t)$ can be fully recovered (see the dashed red curve in Fig. S4). For the last half of $f(t)$ which has similar decreasing trend as $g(t)$, if we deconvolve it with $g(t)$, the obtained excitation time series is totally different with the inputted $e(t)$ (see the dashed light blue curve in Fig. S4).

Here are the problems coming. DH20 claimed that *'However, if it is the latter case, then the output series via the continuous stochastic excitation may be various with the different input series*

(e.g., supplementary Fig.18), that is to say, if the output result (or the original observed signal) is decaying, then the result recovered by our method will be decreasing as well', so which part of the output will be used to recover the signal? From their Fig. 18, most of the last half of the output are decreasing.

If the observed EYO is increasing as DH20 suggested, and it was continuously excited, can we believe that the EYO must be an increasing normal mode? As the SYO also has similar relationship with jerks as DH20 suggested for EYO, following them, we can also suggest that SYO was continuously excited. So if we use jerk excitation for the increased EYO amplitude as DH20 suggested, how to explain the decreased SYO amplitude? Should it be increased as the EYO?

In summary, for the real world, only from the fluctuation characteristics of a signal in the time-domain, no matter it has damping amplitude, oscillation amplitude or even stable amplitude, without other independent information, one cannot definitely claim anything about its excitations or attenuation Q .

Reference

1. Duan, P., Huang, C. (2020) Intradecadal variations in length of day and their correspondence with geomagnetic jerks. *Nat. Commun.* 11, 2273. Doi: 10.1038/s41467-020-16109-8.
2. Chao, B.F. (2017) On rotational normal modes of the Earth: resonance, excitation, convolution, deconvolution and all that. *J. Geod. Geodyn.* 8 (6), 371–376.